Formation of African Easterly Waves and Mesoscale Convective Systems over Eastern Africa and its Implication to Tropical Cyclogenesis over Eastern Atlantic Ocean

AIP Conf. Proc. -- July 6, 2009 -- Volume 1140, pp. 104-113
PROCEEDINGS OF THE NATIONAL SOCIETY OF BLACK PHYSICISTS: 35th Annual Day of Scientific Lectures & 31st Annual Meeting, 2008 Joint Annual Conference of The National Society of Black Physicists and The National Society of Hispanic Physicists;
DOI:10.1063/1.3183511

Issue Date: 6 July 2009

ABSTRACT

Yuh-Lang Lin
Department of Physics/Energy and Environmental Studies, North Carolina A&T State University Greensboro, North Carolina 27411

The formation of African easterly waves and mesoscale convective systems in eastern North Africa and its impacts on the tropical cyclogenesis over the eastern Atlantic Ocean is studied. Based on numerical simulations, AEWs can be produced by vortex shedding from the EH. The lee vortex is generated mainly by the blocking of the EH and helped by the horizontal shear associated with the northeasterly wind and the jet passing through the Turkana channel. The MCS was originated from the moist convection over the EH triggered by diurnal sensible heating. When the MCS moved to the lee of the mountain, it merged with the lee vortex of the AEW train and formed the coupled AEW-MCS system. Numerical simulations of a regional climate model indicate that the simulated fields do possess the AEW characteristics and the convection was generated over the EH, and the pre-Alberto AEW-MCS system was generated near the lee of the EH. Finer-resolution numerical simulations demonstrate that the vortex generated on the lee and MCS over the mountain eventually merge and become an AEW-MCS system which might serve as a precursor of tropical cyclone. ©2009 *American Institute of Physics*

KEYWORDS and PACS

Keywords

convection, wind, climatology, satellite broadcasting

PACS

- 92.60.hk Convection, turbulence, and diffusion in meteorology
- 92.60.Gn Winds and their effects
- 92.05.Df Climate and inter-annual variability in oceanography
- 95.40.+s Artificial Earth satellites
- YEAR: 2009

PUBLICATION DATA

Formation of African Easterly Waves and Mesoscale Convective Systems over Easterm Africa and its Implication to Tropical Cyclogenesis over Eastern Atlantic Ocean

Yuh-Lang Lin

Department of Physics/Energy and Environmental Studies
North Carolina A&T State University
Greensboro, North Carolina 27411

Abstract. The formation of African easterly waves and mesoscale convective systems in eastern North Africa and its impacts on the tropical cyclogenesis over the eastern Atlantic Ocean is studied. Based on numerical simulations, AEWs can be produced by vortex shedding from the EH. The lee vortex is generated mainly by the blocking of the EH and helped by the horizontal shear associated with the northeasterly wind and the jet passing through the Turkana channel. The MCS was originated from the moist convection over the EH triggered by diurnal sensible heating. When the MCS moved to the lee of the mountain, it merged with the lee vortex of the AEW train and formed the coupled AEW-MCS system. Numerical simulations of a regional climate model indicate that the simulated fields do possess the AEW characteristics and the convection was generated over the EH, and the pre-Alberto AEW-MCS system was generated near the lee of the EH. Finer-resolution numerical simulations demonstrate that the vortex generated on the lee and MCS over the mountain eventually merge and become an AEW-MCS system which might serve as a precursor of tropical cyclone.

Keywords: African easterly wave (AEW), mesoscale convective system, tropical cyclone (TC), AEW-MCS, Ethiopian Highlands, mesoscale convective complex, African easterly jet (AEJ), Turkana Channel.
PACS: 90

INTRODUCTION

It is well recognized that a preexisting cyclonic disturbance is needed to initiate tropical cyclones (TCs). African easterly waves (AEWs) that emerge from the West African coast are a known precursor for the TCs generated in the vicinity of the Cape Verde Islands over the eastern Atlantic Ocean. AEWs account for about 60% of the Atlantic basin tropical storms and nonmajor hurricanes, and about 85% of major hurricanes[3]. These disturbances could begin developing into TCs before emerging from western Africa.

It has been proposed[4] the possibility that easterly waves may develop downstream of the Ethiopian Highlands (EH) as a result of orographic influence on the easterly flow. On the other hand, it has been argued[5] that easterly waves do not exist before reaching the EH and do not develop immediately downstream of the EH. In addition, two AEW paths are identified: one propagates along the Saharan thermal low near 20^{o}N, which is located to the north of the African easterly jet (AEJ) at about 925 mb; the other propagates near 10^{o}N at about 600 mb. The northern AEW path is generally

accompanied by the convergence of the surface Harmattan northeasterlies and the surface monsoon southwesterlies, while the southern AEW path is generally located to the south of the AEJ.

It has been shown numerically that mountains in northcentral Africa may also generated AEWs. In fact, the pre-Alberto (2000) disturbance could be traced back in time to the lee of the EH, a mountain located further to the east[1] (Fig. 1). it is found[1,2] that 23 out of 34 pre-TC AEWs over eastern Atlantic for the period of 1990 to 2001 were generated from EH. In addition, the MCS went through several life cycle of genesis and lysis when it crossed the African continent.

On the other hand, it was proposed[6] that the pre-Alberto AEW-MCS system was generated over the Darfur Mountains (DM) of Sudan. Thus, mountains in the eastern Africa are able to generate AEWs and their associated MCS for triggering TCs off the west coast of Africa. However, further studies are required to clarify the roles EH and DM plays in generating the AEWs and their embedded MCSs.

FORMATION MECHANISMS OF AEW

Several mechanisms have been proposed to explain the formation of AEWs in the past: (1) barotropic-baroclinic instability, (2) baroclinic instability of shallow low static stability associated with Saharan surface heating, (3) condensational heating, (4) AEJ and orographic forcing associated with mountains in northcentral Africa, (5) orographic forcing associated with mountains in eastern Africa, and (6) cumulus convection embedded in the ITCZ. Thus, the relative roles played by the instabilities, surface sensible heating, elevated latent heating, AEJ and mountains on the formation of AEWs are still not quite clear.

Based on the above discussed mechanisms and previous studies[1,2,6], we hypothesize that

(1) AEWs generated in eastern North Africa are mainly generated by the vortex shedding associated with EH and its surrounding topography,
(2) Horizontal shear and jet through the Turkana Channel help strengthen the lee vortex produced by EH,
(3) Initial convection over EH and DM is produced by diurnal heating, and
(4) The MCS and AEW then merge into a coupled AEW-MCS system on the lee of EH or DM.

In order to test the above hypothesis on the formation of AEWs, we first employed the Coupled Ocean/Atmosphere Mesoscale Prediction System (COAMPS^{TM})[13] to conduct an idealized simulation of uniform, easterly flow encountering bell-shaped topography representative of the EH in an environment devoid of moisture, surface radiation, and the planetary boundary layer processes. Using this approach, we are able to isolate the orographic effects from other complicated physical processes. The COAMPS model features non-hydrostatic, fully compressible primitive equations calculated with the Arakawa and Lamb C-grid scheme and with 2nd-order, centered-time differencing. Full details of the COAMPS model, along with relevant references, can be found within the COAMPS model description[13].

For the idealized simulation conducted here, basic zonal wind is specified as $U = -10$ ms^{-1} throughout the model domain, which extends to 15 km in depth. Complications from the effects of weak baroclinicity observed over the EH region are avoided with the specification of uniform flow; baroclinic effects will be covered in a separate paper. The profile of wind and temperature (Fig. 2) used to initialize the simulation reflects the respective 1-day composite profile calculated from EOM data at 15.0ºN, 42.5ºE -- a position centered over the Red Sea (Fig. 3).

The EH topography is idealized as a three-dimensional bell-shaped mountain as:

$$h = h_0\left(\frac{x^2}{a^2} + \frac{y^2}{b^2} + 1\right)^{-3/2}, \qquad (1)$$

where h is the height of the idealized topography calculated at point (x, y) relative to the topography center, h_o is the maximum height centered at $(x, y) = (0, 0)$, a and b are the half-widths of topography in the x and y directions, respectively. For this simulation, h_o = 3.5 km, a = 100 km, and b = 300 km, which gives bell-shaped topography oriented lengthwise against the prescribed easterly flow.

The model domain is specified as a horizontal grid of 161×121 points with a spatial resolution of 50 km, and with 30 σ-z vertical levels spaced every 500 m. The domain is prescribed with parameters of $f_o = 2.526\times10^{-5}$ s^{-1} and $\beta = 2.248\times10^{-11}$ s^{-1}m^{-1}, translating to a β plane surrounding φ_o = 10ºN. The model simulation is integrated with a time step of Δt = 60 s over a period of 180 h (7.5 d). The lateral boundaries of the model domain employ the radiation condition, which allows the disturbance generated within the domain to propagate through these boundaries.

Figure 4 shows the potential vorticity (PV) and streamline fields of the dry simulation for t = 1d, 3d, 5d, and 7d. After day 1 (Fig. 4a), flow upstream of the idealized topography is blocked and redirected around the topography. A pair of cyclonic and anticyclonic PV maxima is produced to the north and south, respectively, at the lee side of the idealized EH. Without the effects of friction and latent heating in this model simulation, the relative vorticity field is similar to the PV field. Early in the simulation, vorticity generation on the lee side of the idealized EH may be a result of baroclinic vorticity tilting when the PV is conserved and by the generation of PV through numerical dissipation at later stages when the PV is not conserved[7]. Note that the Froude number (U/Nh) in this case is about 0.260 (based on U = 10 ms^{-1}, N = 0.011 s^{-1} and h_o = 3500 m), indicative of the low-Froude number regime for lee vortex generation in an inviscid fluid[7]. A hydrostatic mountain wave is produced over the idealized EH along y = 500 km, where the flow is able to climb over the mountain an fall down the lee slope (Fig. 5 – left panel). The Coriolis effect is significant enough to allow positive PV anomalies to grow more over time than negative PV anomalies, as observed in previous studies of low-Froude number flow passage over a mesoscale mountain in an f-plane environment[7]. This tendency of greater positive PV development can be seen for t = 3d, 5d, and 7d (Figs. 4b-d).

Once a positive PV anomaly has developed at the northern and lee quadrant of the idealized EH and propagates downstream, the perturbed flow adjusts toward restoration of its original pattern; overadjustment allows for the generation of the

second positive PV anomaly at day 3 (Fig. 4b). Due to the strong blocking associated with low Froude-number flow, the positive PV anomaly at the lee side of the idealized EH becomes a cyclonic vortex. Instead of simple vortex shedding in non-rotating, inviscid fluid flow in which symmetric, alternate positive and negative PV anomalies are generated[7], vortices shed from the idealized EH are predominately cyclonic. At day 5 (Fig. 4c), the first vortex or PV has become solitary and propagates to approximately x = -3000 km. At this time, a third vortex or positive PV is forming at the northern, lee quadrant of the idealized EH. At day 7, there are three identifiable vortices aligned along y = 500 km. These lee vortices form a wave train separated by a distance of about 2000 km, which is comparable to the wavelength of the AEW train (2200 km) described earlier and of formerly observed AEWs (2000-4000 km)[8]. The propagation speed of the idealized EH-generated easterly waves is about 7.9 m s^{-1}, which is slower than the basic wind speed (10 ms^{-1}) and the phase speed of the aforementioned AEW train (11.6 ms^{-1}), but comparable to previously observed AEWs (7 - 9 ms^{-1})[8].

The wave properties may also be revealed from vertical cross sections of potential temperature and PV fields at y = 500 km (Fig. 5 – left panel). The lee vortices are each associated with a warm region (dipping of the isentropes) and positive PV. The positive PV anomaly associated with the vortex develops exclusively from positive vorticity generation, since no latent heating or friction is included in the simulation. The warm anomaly associated with each vortex originates from adiabatic warming of the downslope wind as the vortex forms (Fig. 4). The distance separating each warm anomaly is approximately 2000 km. The right panel of Fig. 5 shows the perturbation meridional wind fields simulated by the COAMPS model at y = 500 km. As shown with the vorticity field (Fig. 4) and with the vertical velocity field (Fig. 5 – right panel), a wave-like disturbance is evident in the meridional wind field. The simulated meridional wind field compares well with EOM analysis of the pre-Alberto disturbance (not shown) and with past observational studies. With the absence of any heating source, easterly waves generated at the idealized EH are confined to the lower troposphere by low Froude number conditions. Hence, these easterly waves would fall under the classification of a forced equatorial Rossby wave[9]. The simulated vertical velocity field is quite weak, implying that the warm anomalies associated with the propagating lee vortices and easterly waves are generated from adiabatic warming at, and then advected from, the lee slope of the idealized EH.

FORMATION OF A COUPLED MCS-AEW SYSTEM

AEWs usually are comprised of one or more MCSs[10]. Occasionally, MCSs may develop into TCs. When one or more large, well-organized MCS initially develops, several mesoscale vortices (MVs) can be found within the convective systems. In the study about a warm-core vortex developed from an MCS[11], the vortex was found to be instrumental in the development of new MCSs, thus sustaining the MCS-MV system. The environmental conditions surrounding MVs and the accompanying MCSs/MCCs are similar to those of TCs, though MCSs or MCCs are more commonly found over land. The similar environmental conditions would explain the propensity of MCSs to give rise to, and become a component of,

a TC. This idea[10] was illustrated by tracing three TCs from MCSs in western Africa, and the MCSs themselves developed in the African Sahel. In fact, MCSs were prone to develop near regions with high topography. One example is the pre-Alberto (2000) AEW-MCS system, which was traced back to the EH[2].

Initial convection for the pre-Alberto AEW-MCS system began over the peaks of the northern EH during the local afternoon of 28 July 2000 (Fig. 6a)[12]. After dark, the convective cells continued to grow as they tracked westward (Fig. 6b). By 2200 UTC 28 July 2000, growing convective cells from Eritrea moved southwestward and combined with westward-moving cells from northern Ethiopia, resulting in the development of an MCC (Fig. 6c). As the local nighttime progressed, the MCC peaked and began to diminish as it propagated in a southwestward and even southward direction (Fig. 6d). With the convection continuing to diminish, the overall cloud feature resumes a more westward track (Fig. 6e). From the residual clouds, an MV becomes evident over central Sudan at 1600 UTC 29 July 2000 (Fig. 6f). From that time, the MV would continue westward and contribute to the generation of a larger MCC over southern Chad; the National Hurricane Center first recognized the AEW by this cloud signature in a post-mortem tropical cyclone report.

A 3-day average of the 850-hPa mixing ratio and wind from ECMWF operational model data, surrounding the time of observed MCC development, shows the most significant advection of low-level moisture near the west slopes of the EH from the southwest (Fig. 7). Not only is moisture readily available for convective development over and to the west of the EH, the direction of moisture advection promotes leftward propagation of convective cells relative to the mean-layer (northeasterly) flow (Fig. 8), as occurred with the northernmost and most vigorous convection observed in the presented case.

Figure 9 shows numerically simulated convective cells, which are forced by diurnal sensible heating, and a lee vortex, as part of the AEW, are able to merge into a AEW-MCS system.

CONCLUDING REMARKS

Based on idealized numerical modeling simulations, we are able to demonstrate that AEWs can be generated by the vortex shedding associated with an idealized EH. Based on reanalysis data, there is evidence that horizontal shear and jet through the Turkana Channel are able to help strengthen the lee vortex produced by EH. A finer-resolution numerical simulation has shown that the vortex shed from EH is able to merge with the convective cells produced by sensible heating over the mountains on the lee of the EH, thus forms an AEW-MCS system.

The above processes need to be revisited by adopting a single modeling system to test the proposed hypothesis systematically. The relative roles played by the EH and DM on the formation of the AEW-MCS system still need to be investigated.

ACKNOWLEDGMENTS

The help from Chris Hill and Katie Robertson is appreciated. This research is supported by the Office of Naval Research (Grant No. N00014-02-1-0674).

REFERENCES

1. C. M. Hill and Y.-L. Lin, *Geophys. Res. Lett.*, **30**, 1232, doi:10.1029/2002GL016655 (2003).
2. Y.-L. Lin, K. E. Robertson, and C. M. Hill, *Mon. Wea. Rev,* **133***,* pp. 3276-3298 (2005).
3. S. B. Goldenberg, C. W. Landsea, A. M. Mestas-Nunez, and W. M. Gray, *Science*, **293**, pp. 474-479 (2001).
4. N. L., Frank, *Mon. Wea. Rev*., **98**, pp. 307-314 (1970).
5. R. W. Burpee, R. W., *J. Atmos. Sci.*, **29**, pp. 77-90 (1971).
6. G. J. Berry and C. Thorncroft, Mon. Wea. Rev., **133**, pp. 752-766 (2005).
7. Y.-L. Lin, *Mesoscale Dynamics*, Cambridge, UK, Cambridge University Press, 2007, 630pp.
8. R. J. Reed, Norquist, Donald C., Recker, Ernest E., *Mon. Wea. Rev*., **105**, 317–333 (1977).
9. J. R. Holton, J. R., *Mon. Wea. Rev.*, **98**, pp. 614-615 (1970).
10. A. G. Laing, A. G. and J. M. Fritsch, *Mon. Wea. Rev.*, **121**, pp. 2254- 2263 (1993).
11. J. M. Fritsch, J. D. Murphy, and J. S. Kain, *J. Atmos. Sci.*, **51**, pp. 1780-1807 (1994).
12. C. M. Hill and Y.-L. Lin, Hurricane Conference, Amer. Meteor. Soc. (2006).
13. S. Chen, J. Cummings, J. Doyle, R. Hodur, T. Holt, C. S. Liou, M. Liu, J. Ridout, J. Schmidt, W. Thompson, A. Mirin, and G. Sugiyama, Naval Research Laboratory Tech. Report, NRL/PU7500-04-448, 2003, 141pp.

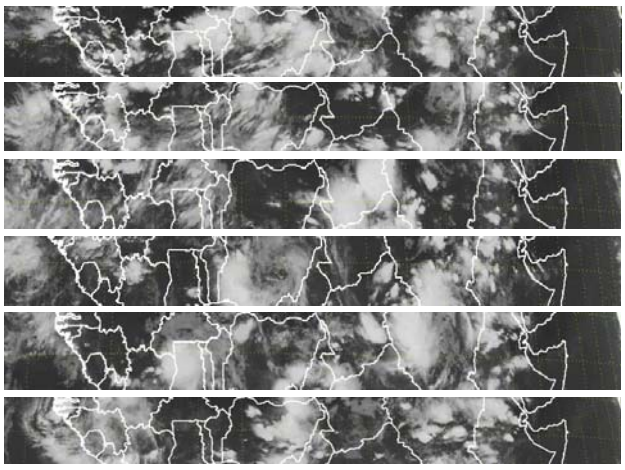

FIGURE 1. Time-longitude section of METEOSAT-7 infrared satellite imagery for 1800 UTC 28 July 2000 through 1800 UTC 02 August 2000 every 24h. Area depicted is approximately (5ºN - 15ºN) × (25ºW -60ºE)^2. Imagery is from EUMETSAT.

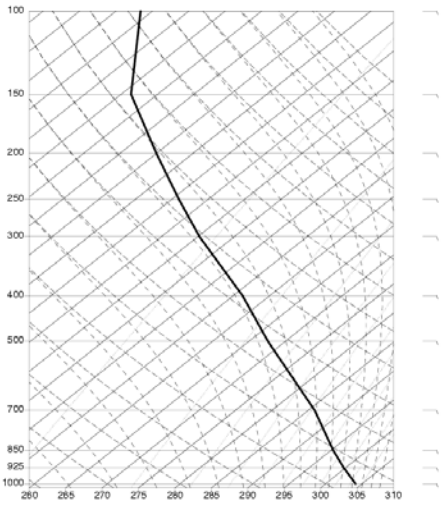

FIGURE 2. A composite sounding of EOM temperature data and of prescribed wind field (U = -10 m s^{-1}) used for the idealized simulation. Temperature is averaged for 0000, 0600, 1200 and 1800 UTC 27 July 2000 at 15.0ºN, 42.5ºE, located to the northeast of EH over the Red Sea.

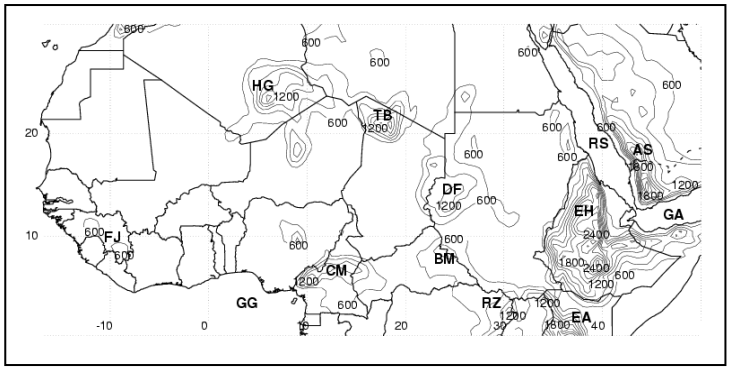

FIGURE 3. Terrain data as resolved from ECMWF Operational Model data set. Terrain is contoured every 600 m. Labels indicate geographical features of Africa, which are defined as: AS: Asir Mountains; BM: Bongo Massif; CM: Cameroon Highlands; DF: Darfur Mountains; EA: Eastern Arc Mountains; EH: Ethiopian Highlands; FJ: Futa Jallon Highlands; GA: Gulf of Aden; GG: Gulf of Guinea; HG: Hoggar Mountains; RZ: Ruwenzori Mountains; TB: Tibesti Mountains.

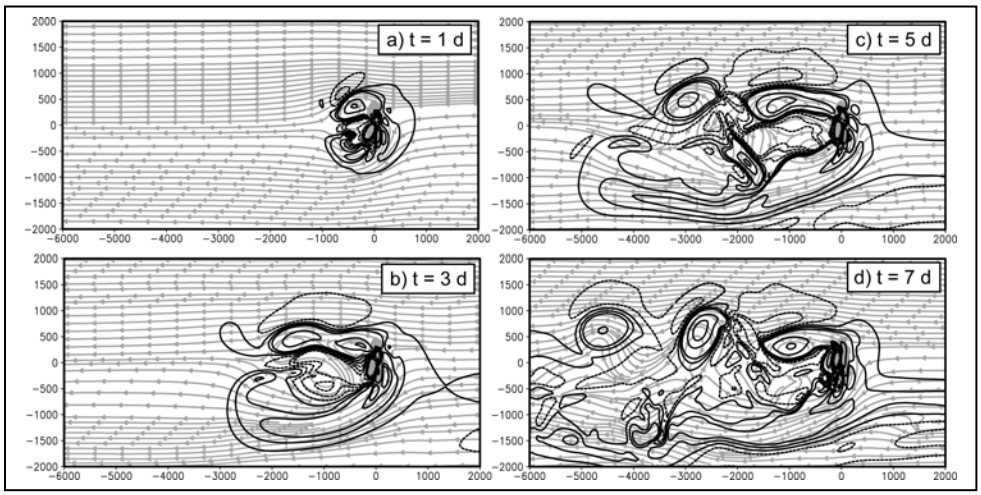

FIGURE 4. COAMPS streamline and potential vorticity (*PV*) fields for (a) t = 1 d, (b) t = 3 d, (c) t = 5 d, and (d) t = 7 d. Bell-shaped terrain higher than 0.5 km, centered at x = 0 km and y = 0 km, is shaded. *PV* is contoured every 0.04 pvu (PV unit) for -0.10 pvu ≤ PV ≤ 0.10 pvu and every 0.20 pvu for PV < -0.10 pvu and PV > 0.10 pvu. Positive (negative) PV is denoted by solid (dotted) contour.

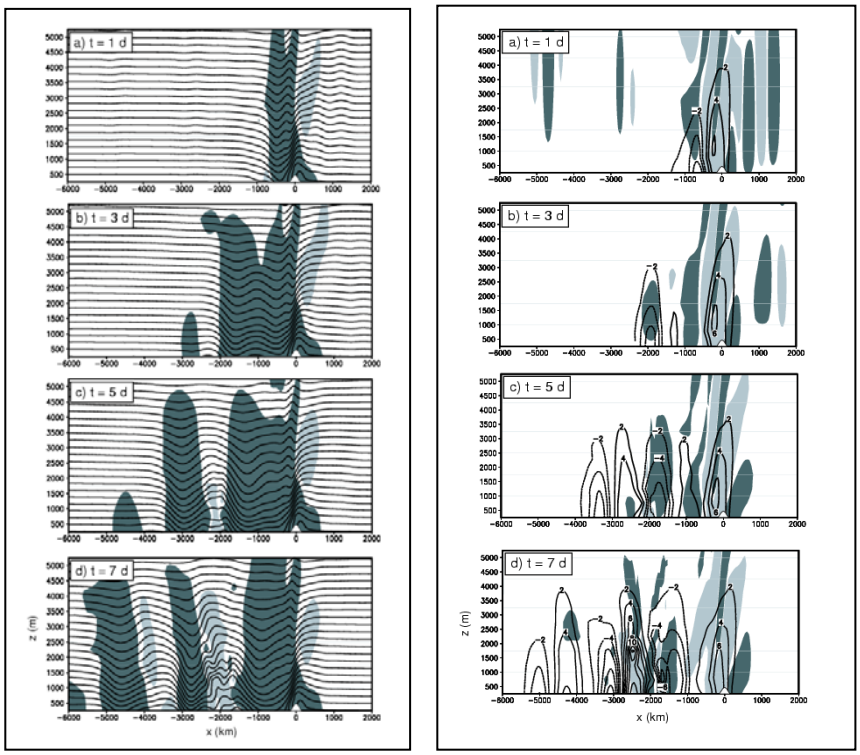

FIGURE 5. Left panel: The vertical cross section at y = 500 km of COAMPS potential temperature (θ) and potential vorticity (*PV*) fields for (a) t = 1 d, (b) t = 3 d, (c) t = 5 d, and (d) t = 7 d. Regions of $PV \geq$ 0.02 pvu are heavily shaded, while regions of $PV \leq$ -0.02 pvu are lightly shaded. Right panel: Same as left panel except for the meridional (v) and vertical wind (w) velocity fields. Southerly (northerly) winds are denoted by solid (dotted) contours. The v-wind speed contour is 2 m s^{-1}. Regions of $w \geq 2$ mm s^{-1} are heavily shaded, while regions of $w \leq$ -2 mm s^{-1} are lightly shaded.

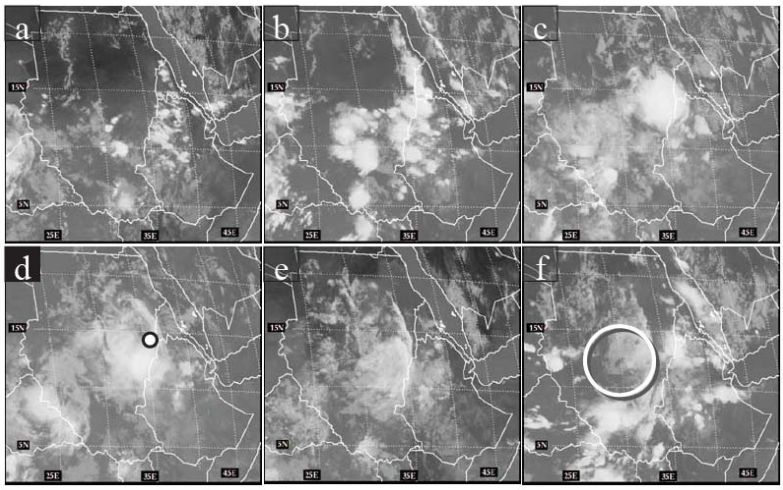

FIGURE 6. METEOSAT-7 infrared-wavelength imagery for a) 1200 UTC 28, b) 1600 UTC 28, c) 2200 UTC 28, d) 0400 UTC 29, e) 1000 UTC 29, and f) 1600 UTC 29 July 2000. Dot in d) depicts previous MCC center of c). Circle in f) encompasses visible MV. Imagery provided by EUMETSAT @ 2003[12].

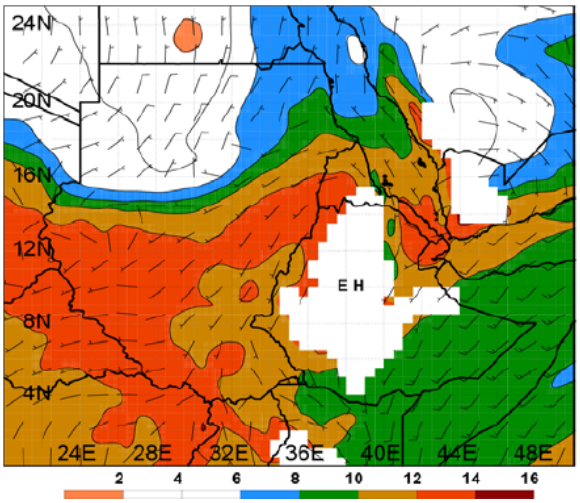

FIGURE 7. ECMWF 3-day composite analysis of 850-hPa water vapor mixing ratio (g kg^{-1}) for 27 to 29 July 2000[12]. Contours every 2 g kg^{-1}.

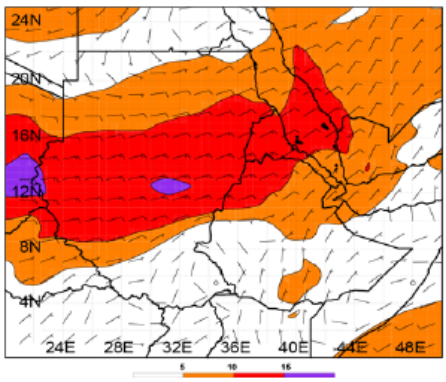

FIGURE 8. ECMWF 3-day composite analysis of 600-hPa wind (ms^{-1}) for 27 to 29 July 2000[12]. Contours every 2 g kg^{-1}.

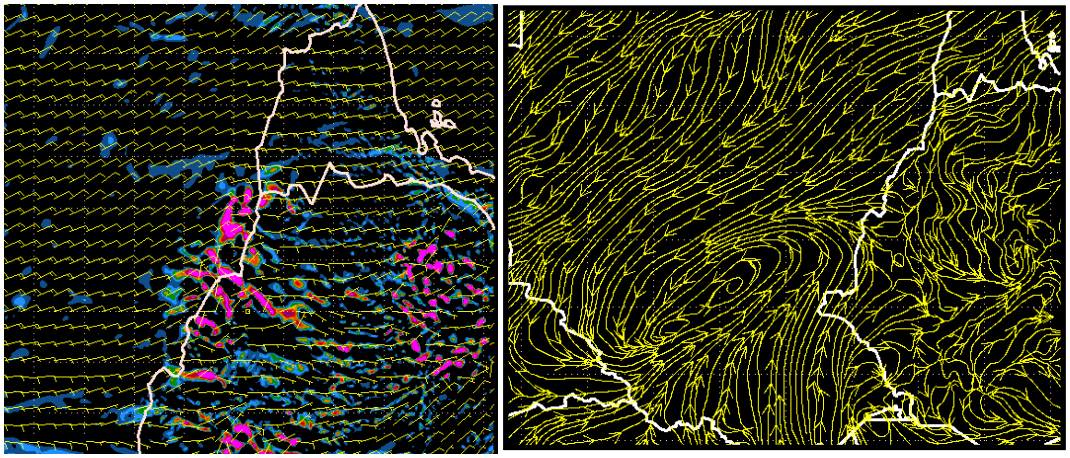

FIGURE 9. Numerically simulated convective cells and lee vortex are collocated on the lee of EH to form an AEW-MCS system as a precursor for Hurricane Alberto (2000)[12].